Kinetics of the Oxidative Coupling of Methane at Atmospheric Pressure in the Absence of Catalyst

Qi Chen, Jozef H. B. J. Hoebink, and Guy B. Marin*

Laboratorium voor Chemische Technologie, Eindhoven University of Technology, P.O. Box 513, 5600 MB Eindhoven, The Netherlands

Continuous flow experiments for the oxidative coupling of methane in the absence of catalyst and at low methane conversion were carried out in empty tubular quartz reactors at atmospheric pressure, temperatures from 873 to 1123 K, and inlet molar ratios of CH_4/O_2 from 4 to 10 and of He/CH_4 from 0 to 1.25. The methane conversion varied from 2 to 15% and the oxygen conversion from 10 to 100%. A reaction network was constructed on the basis of elementary free-radical reactions. Arrhenius parameters were estimated for the most important reactions by regression of experimental data. The effects of the process conditions on the conversions of methane and oxygen as well as on the selectivities toward products were simulated adequately by considering 33 elementary reactions. Ethane is mainly formed from the recombination of methyl radicals arising from degenerate branched chains involving OH and HO_2 as main chain carriers. Ethene originates from ethane mainly via a pyrolytic chain, while the oxidative dehydrogenation contributes to a much lower extent. Carbon monoxide originates from the oxidation of methyl radicals, whereas the contribution of the consecutive oxidation is not significant at the conversion levels investigated.

Introduction

The oxidative coupling of methane aimed at the production of higher hydrocarbons has attracted much attention during the past years. This reaction is usually carried out in the presence of catalysts and requires temperatures up to 1150 K. At these temperatures, noncatalytic reactions in the gas phase, however, play an essential role in the formation of higher hydrocarbons. It is generally accepted that the most widely studied alkali metal/alkaline earth metal oxide and the rare earth metal oxide catalysts act as a methane activator and in particular as a producer of methyl radicals, with the subsequent reactions taking place in the gas phase (Ito et al., 1985). Whether or not the reducible multivalent metal oxides catalyze the reactions in the same way is still in debate.

The importance of the gas-phase reactions has been well recognized and is reflected in several recent papers on the oxidative coupling of methane in the absence of catalyst (Labinger and Ott, 1987; Lane and Wolf, 1988; Geerts et al., 1990; Zanthoff and Baerns, 1990). Furthermore, in a recent review, Lunsford (1990) has pointed out the importance of branched-chain reactions in the gas phase with respect to the generation of methyl radicals. Consequently, Lunsford proposed that catalysts might be an important initiator of the chain reaction, but not a major source of methyl radicals. Kinetic models based on the free-radical mechanism have been set up in order to understand the role played by the gas-phase reactions and the interaction between the gas-phase reactions and the reactions on the catalyst surface. The Arrhenius parameters were selected from data bases in the literature that originate mainly from combustion kinetics (Tsang and Hampson, 1986; Warnatz, 1984). While the dependence of the coupling selectivity on conversion has been described adequately, the experimentally observed dependence of the methane and oxygen conversions on space time has not been accounted for successfully. Typically, the methane conversion rate observed at 1273 K is about 4 orders of magnitude higher than calculated (Lane and Wolf, 1988). One exception is the work by Kimble and Kolts (1987), who set up a model consisting of a methane activation through a hydrogen abstraction by the catalyst surface and a number of subsequent free-radical reactions among the hydrocarbons without involving any oxygen-containing species. With this model, the methane conversion as well as C_{2+} selectivities were calculated. Good agreement between the model prediction and experiments was obtained for the dependence of conversion and selectivities on time. Naturally, the dioxygen conversion and the CO_x selectivities could not be calculated.

Since the kinetic parameters in the literature vary by orders of magnitude, choosing the appropriate values is not trivial. The reported parameters might have been determined for conditions widely different from those of interest to the oxidative coupling of methane. Combustion temperatures amount to 2000 K, whereas the highest temperature in the oxidative coupling of methane is below 1200 K and can even be as low as 900 K. Estimating appropriate Arrhenius parameters by regression analysis of experimental data should lead to better results. This approach has widely been applied in kinetic studies of heterogeneous catalytic reactions (Froment and Hosten, 1981).

The present study attempts to establish a detailed kinetic model for the oxidative coupling of methane at atmospheric pressure in the absence of catalyst and to determine a set of reliable Arrhenius parameters for the elementary radical reactions involved under these conditions by careful selection from data bases and by means of the regression of experimental data obtained in our laboratory. The important chains, branched or nonbranched, which lead to the formation of the major products, are identified.

Procedures

Experiments. The setups used for the experiments and the experimental procedures have been described in detail elsewhere (Van Kasteren et al., 1988). The reactors consisted of empty quartz tubes with dimensions ranging from 160 mm in length and 6 mm in diameter to 400 mm in length and 10 mm in diameter. A thermocouple well in the axis of the reactor allowed the measurement of the axial temperature profile during reaction. The temperature profile is of a parabolic shape, and the difference between the highest temperature and the inlet or outlet temperature can be over 400 K. This profile was accounted for during the regression. The reactor was heated electrically by a ceramic tubular oven.

0888-5885/91/2630-2088$02.50/0 © 1991 American Chemical Society

Table I. Experimental Conditions

temperature, K	873–1123
pressure	atmospheric
molar ratio $CH_4/O_2\|_0$	4–10
molar ratio $He/CH_4\|_0$	0–1.25
space time $V/F_{CH_4,0}$, m^3 s mol^{-1}	0.1–1.9

The analysis of the reactor effluent was performed by means of on-line gas chromatography (GC). Two samples were taken from the reactor effluent. In one sample, hydrogen, methane, oxygen, and carbon monoxide were separated by a column packed with molsieve-5A and detected by a thermal conductivity detector (TCD). In the second sample, methane, carbon dioxide, water, and the other hydrocarbons were separated by a column packed with Porapak-R and detected by a second TCD.

The experiments covered a range of conditions summarized in Table I. In some experiments, helium was used as an inert diluent to lower the partial pressures of methane and oxygen. In total, the results of 20 experiments were taken.

The fractional conversion of methane, X_{CH_4}, or oxygen, X_{O_2}, is defined as

$$X_{CH_4} = \frac{F_{CH_4,0} - F_{CH_4}}{F_{CH_4,0}} \qquad \text{(eq 1)}$$

$$X_{O_2} = \frac{F_{O_2,0} - F_{O_2}}{F_{O_2,0}} \qquad \text{(eq 2)}$$

The selectivity for product j with respect to methane, S_{j,CH_4}, or oxygen S_{j,O_2}, is defined by the following ratios:

$$S_{j,CH_4} = \frac{n_j(F_j - F_{j,0})}{F_{CH_4,0} - F_{CH_4}} \qquad \text{(eq 3)}$$

$$S_{j,O_2} = \frac{m_j(F_j - F_{j,0})/2}{F_{O_2,0} - F_{O_2}} \qquad \text{(eq 4)}$$

with n_j and m_j the number of carbon and oxygen atoms respectively in product j.

A 100% carbon balance between the reactor inlet and outlet streams was assumed. This allowed calculation of the molar flow rates of the components at the reactor outlet starting from the GC analysis. All conversions and selectivities were determined on this basis, including the conversion of oxygen and the selectivities with respect to oxygen.

Reactor Model. No energy equation was needed for the reactor model, because the measured axial temperature profile was accounted for and the radial temperature gradients were negligible. The latter statement was justified by the following criterion valid for the empty tubular reactors and derived in a way analogous to that of Mears for fixed bed reactors (Mears, 1971):

$$\frac{|\Delta H^\circ_r R_v| d_t^2}{\lambda_e T} < 3.2\frac{RT}{E_a}$$

with ΔH°_r standard enthalpy of reaction (J mol^{-1}); R_v, volumetric production rate of methane (mol m^{-3} s^{-1}); d_t, reactor tube inner diameter (m); λ_e, effective heat conductivity (W m^{-1} K^{-1}); and E_a, activation energy in the global rate equation describing the disappearance of methane (J mol^{-1}).

When this relation is satisfied, the difference between the reaction rate at the wall and the average rate over the cross section corresponding to the hot spot in the reactor is less than 10%. Even in the most conservative hypothesis, i.e., a rate of methane disappearance of 1.0 mol m^{-3} s^{-1} and molecular heat conductivity, the above criterion is satisfied.

The pressure drop over the reactor was negligibly small. Therefore, the reactor model is reduced to a set of continuity equations for the species involved. The flow pattern in the reactor is assumed to be of the plug flow type. With these assumptions, the continuity equation for component j at the steady state is given by

$$\frac{dF_j}{dz} = \frac{\pi d_t^2}{4}\sum_i \nu_{ij} r_i \qquad \text{(eq 5)}$$

with F_j, molar flow rate of the jth component (mol s^{-1}); z, length along the reactor (m); ν_{ij}, stoichiometric coefficient of the jth component in the ith reaction, negative for a reactant and positive for a product; and with as initial condition, $F_j = F_{j,0}$ at $z = 0$.

Every reaction consists of both a forward and a backward step. The rate of reaction i, r_i, is given by

$$r_i = \vec{r}_i - \overleftarrow{r}_i = k_i\prod_j C_j^{\alpha_{ij}} - k_{-i}\prod_j C_j^{\alpha_{-ij}} \qquad \text{(eq 6)}$$

in mol m^{-3} s^{-1}, with $\vec{r}_i$ and $\overleftarrow{r}_i$ being the rate of the forward and backward step respectively, k_i and k_{-i} the corresponding rate coefficients, and C_j the concentration of component j in mol m^{-3}. As only elementary steps are considered, the reaction orders, α_{ij} and α_{-ij}, are equal to the molecularities of the involved reactants. Integration of the continuity equations (eq 5) leads to the concentrations of all the involved components. These equations form a stiff set of ordinary differential equations; i.e., the local eigenvalues differ by orders of magnitude. In practice, the concentration change of the active intermediates is much faster than that of the stable molecules. The algorithm developed by Gear has been widely applied for such integrations (Gear, 1971; Sundaram and Froment, 1978). In the present study, two versions of FORTRAN codes of the Gear routine implemented by Hindmarsh (1983) and by the Numerical Algorithm Group (NAG, 1988), respectively, have been tried. Both versions turned out to show divergence at certain conditions. Moreover, long computation times were required. That is why an algorithm more specific for chemical kinetics was employed in the present work (Dente et al., 1979). This algorithm makes use of the pseudo-steady-state approximation for the reactive intermediates. It has been used successfully in kinetic studies of thermal cracking processes (Dente et al., 1979; Clymans, 1982). It reduces computation times by a factor of 10 compared with the Gear algorithm. In addition, it is highly stable.

Regression Analysis. The estimation of the most important kinetic parameters was performed by minimization of the following objective function:

$$S(\mathbf{b}) = \sum_j^{\upsilon} w_j \sum_k^{n} [y_{kj} - f_j(\mathbf{x}_k,\mathbf{b})]^2 \qquad \text{(eq 7)}$$

with $f_j(\mathbf{x}_k,\mathbf{b})$, response value calculated with the model for response j of experiment k; $\mathbf{x}_k$, vector of independent variables; y_{kj}, response values observed experimentally for response j of experiment k; $\mathbf{b}$, parameter vector; υ, the number of responses; n, the number of experiments; and w_j, weighting factor for response j.

This objective function is derived from a simplified form of the generalized least-squares criterion assuming that the experimental errors associated with different responses are uncorrelated. The generalized least-squares criterion results from the maximum likelihood principle, when the experimental errors are normally distributed with a zero mean (Froment and Hosten, 1981). To mimimize the

objective function, a derivative free algorithm from Rosenbrock (Rosenbrock, 1961; Rosenbrock and Story, 1966) was applied in this study. This is a univariable search method; i.e., during the minimization, only one of the parameters is altered at a time.

Only the molar fractions, y_{kj}, of the molecules that were detected accurately at the reactor exit were taken as responses, i.e., dioxygen, methane, carbon monoxide, carbon dioxide, ethyne, ethene, and ethane. Weighting of the responses was performed in order to ensure convergence toward the minimum of the objective function. Methane, with the largest molar fractions in all experiments, is weighted the least. Ethane was given the heaviest weight, 3 orders of magnitude higher than that of methane. The weightings of oxygen and carbon monoxide were 1 order of magnitude higher, whereas those of carbon dioxide, ethyne, and ethene were 2 orders higher, when compared to methane. With these weighting factors, the contribution of each response to the objective function is comparable.

The regression analysis was performed with a detailed reaction network, but only the Arrhenius parameters of the most important reactions were adjusted. The importance of a reaction was assessed with the help of a sensitivity and a contribution analysis.

Sensitivity Analysis. This technique is used frequently in the detailed kinetic modeling of complex chemical reactions, such as the oxidation of methane. By definition, a linear sensitivity factor, ψ_{jkl}, of component j in experiment k with respect to parameter l can be calculated according to

$$\psi_{jkl} = \partial \ln y_{jk} / \partial \ln b_l \qquad \text{(eq 8)}$$

with y_{jk} being the response of component j in experiment k and b_l the lth parameter. The sensitivity analysis discloses the changes of a response brought about by the perturbation of the kinetic parameters, thus connecting the prediction of the model with the rate coefficients of the reactions in the model. This information is useful in elucidating the importance of reactions leading to products and in comparing the relative importance of every elementary step with respect to the product distribution.

Contribution Analysis. A contribution analysis was carried out in addition to the sensitivity analysis. The differential disappearance contribution factor of step i toward the disappearance of component j in experiment k is defined as the ratio of the rate of disappearance of j resulting from reaction i, r^{d}_{ijk}, to the total rate of disappearance of j at a certain position inside the reactor, i.e., at a certain composition of the reaction mixture:

$$\phi^{d}_{ijk} = r^{d}_{ijk} / \sum_i r^{d}_{ijk} \qquad \text{(eq 9)}$$

Here, r^{d}_{ijk} is equal to $\alpha_{ij}\bar{r}_i$ when j appears on the left side of a reaction and to $\alpha_{-ij}\bar{r}_i$ when j appears on the right. Similarly, the differential formation contribution factor can be calculated by using the rates of steps in which component j is formed:

$$\phi^{f}_{ijk} = r^{f}_{ijk} / \sum_i r^{f}_{ijk} \qquad \text{(eq 10)}$$

with r^{f}_{ijk} equal to $\alpha_{-ij}\bar{r}_i$ when j appears on the right side of the reaction and to $\alpha_{ij}\bar{r}_i$ when j appears on the left. Integral contribution factors can also be defined by using rates integrated over the reactor instead of local rates. Calculations showed that the differential contribution factors based on the local rates at the position where $T = T_{max}$ are not significantly different from the integral contribution factors. This is due to the fact that the contribution to the integrated rates over the reactor comes mainly from the middle section of the reactor, where the temperature is higher than the rest of the reactor and close to the maximum temperature. It is expected that the differential contribution factors calculated at the initial stage of the reactions, i.e., at the initial section of the reactor, will be different from the integral factors. A similar analysis was proposed in the literature for eliminating unimportant reactions in the context of combustion modeling (Warnatz, 1983).

Network Construction and Parameter Estimation

The reaction network includes 20 species, out of which 11 are molecules: dihydrogen, water, hydrogen peroxide, dioxygen, methane, methanal, carbon monoxide, carbon dioxide, ethyne, ethene and ethane; and 9 are radicals: hydrogen and oxygen atoms, OH, HO_2, CHO, and CH_3O radicals, and methyl, vinyl, and ethyl radicals.

CH_3CHO was found to be insignificant in a stoichiometric methane–air flame (Warnatz, 1984) and thus excluded from the network. Consequently, two reactive intermediates CH_2CO and CH_3CO, which are related to CH_3CHO, were also excluded. Methanol was not observed in our experiments and is not an important intermediate at the investigated conditions according to the literature. It was not included. Methyl hydroperoxide CH_3OOH is considered to be an important intermediate at temperatures lower than 673 K (Semenov, 1958). It is responsible for the degenerate branching in methane oxidation around that temperature. However, it is much less important at high temperatures (Vardanyan and Nalbandyan, 1985). The present experiments were at significantly higher temperatures; thus this species was omitted. The related radical CH_3O, however, is included, due to its contribution to the methanal formation. Note that radicals CH and its precursor CH_2 were excluded. CH_2 is mainly produced via ethyne. This route has been shown to be minor in the combustion of methane (Warnatz, 1983), and CO formation via these radicals is difficult (Skinner et al., 1972).

A detailed analysis of previously reported reaction models, in particular those presented by Zanthoff and Baerns (1990) and Geerts et al. (1990), leads to a network consisting of 66 reactions among the 20 retained species, as shown in Table II. In what follows, the numbering of the reactions and steps refers to Table II. In this model, heterogeneous reactions such as radical termination by the reactor wall were not included. A simple calculation was carried out to check the importance of the heterogeneous reaction, especially the termination of radicals at the reactor wall. The results showed that, with the conditions and reactors used in the present study, the heterogeneous terminations are controlled by the diffusion of the radicals from the gas bulk to the wall (Boudart, 1968). Hence, the diffusion rate of radicals was taken as the heterogeneous termination rate. Comparison of these rates with the homogeneous termination rates leads to the conclusion that the former can indeed be neglected at the conditions investigated.

The elementary reactions considered can be grouped as follows:

(a) primary initiation, reactions 1 and 2

(b) methyl radical generation, reactions 3–6, in which a radical abstracts a hydrogen atom from methane forming a methyl radical

(c) methyl radical oxidation to CH_3O and CH_2O, reactions 7–10

(d) methyl radical coupling to C_2 components, reactions 11–13

(e) oxidation of CH_3O and CH_2O to carbon monoxide and dioxide, reactions 14–28

Table II. Model for the Oxidative Coupling of Methane in the Absence of Catalyst[a]

no.	reaction	A	n	E_a	A/RT	$\bar{r}$
1	$CH_4 \rightleftarrows CH_3 + H$	0.370E+16		434.00	-4.3	0.164E-04
2	*$CH_4 + O_2 \rightleftarrows CH_3 + HO_2$*	*0.746E+07*		*192.78*	*0.2*	*0.161E-01*
3	*$CH_4 + H \rightleftarrows CH_3 + H_2$*	*0.220E-01*	*3.030*	*43.62*	*0.6*	*0.419E+00*
4	*$CH_4 + O \rightleftarrows CH_3 + OH$*	*0.120E+02*	*2.168*	*62.65*	*14.8*	*0.110E-01*
5	*$CH_4 + OH \rightleftarrows CH_3 + H_2O$*	*0.132E+09*		*33.71*	*3.0*	*0.536E+00*
6	*$CH_4 + HO_2 \rightleftarrows CH_3 + H_2O_2$*	*0.598E+08*		*95.98*	*3.4*	*0.164E+00*
7	*$CH_3 + O_2 \rightleftarrows CH_3O + O$*	*0.781E+09*		*124.80*	*14.2*	*0.434E-01*
8	*$CH_3 + O_2 \rightleftarrows CH_2O + OH$*	*0.536E+08*		*101.00*	*39.4*	*0.441E-01*
9	$CH_3 + OH \rightleftarrows CH_3O + H$	0.864E+09		75.21	0.1	0.371E-06
10	*$CH_3 + HO_2 \rightleftarrows CH_3O + OH$*	*0.804E+08*		*0.00*	*28.9*	*0.135E+00*
11	*$CH_3 + CH_3 \rightleftarrows C_2H_6$*	*0.125E+08*		*0.00*	*4.8*	*0.165E+00*
12	$CH_3 + CH_3 \rightleftarrows C_2H_5 + H$	0.940E+08		108.24	3.9	0.586E-05
13	$CH_3 + CH_3 \rightleftarrows C_2H_4 + H_2$	0.100E+11		134.00	8.8	0.337E-04
14	*$CH_3O \rightleftarrows CH_2O + H$*	*0.158E+15*		*115.00*	*6.0*	*0.178E+00*
15	$CH_3O + O_2 \rightleftarrows CH_2O + HO_2$	0.660E+05		10.90	10.6	0.653E-05
16	$CH_2O + O_2 \rightleftarrows CHO + HO_2$	0.200E+08		163.00	6.2	0.423E-03
17	*$CH_2O + H \rightleftarrows CHO + H_2$*	*0.250E+08*		*16.70*	*6.6*	*0.229E-02*
18	$CH_2O + O \rightleftarrows CHO + OH$	0.350E+08		14.70	20.8	0.675E-03
19	$CH_2O + OH \rightleftarrows CHO + H_2O$	0.580E+08		5.00	9.0	0.203E-02
20	$CH_2O + HO_2 \rightleftarrows CHO + H_2O_2$	0.100E+07		33.50	9.4	0.109E-02
21	*$CH_2O + CH_3 \rightleftarrows CHO + CH_4$*	*0.241E-01*	*2.810*	*22.65*	*6.0*	*0.223E+00*
22	*$CHO + M \rightleftarrows CO + H + M$*	*0.500E+16*	*-2.140*	*85.50*	*7.0*	*0.707E-01*
23	*$CHO + O_2 \rightleftarrows CO + HO_2$*	*0.410E+07*		*0.00*	*11.6*	*0.161E+00*
24	$CHO + CH_3 \rightleftarrows CO + CH_4$	0.120E+09		0.00	11.3	0.813E-03
25	$CO + O_2 \rightleftarrows CO_2 + O$	0.250E+07		200.00	21.5	0.488E-04
26	$CO + O + M \rightleftarrows CO_2 + M$	0.620E+03		12.60	26.5	0.106E-04
27	*$CO + OH \rightleftarrows CO_2 + H$*	*0.440E+01*	*1.500*	*-3.10*	*7.3*	*0.816E-03*
28	*$CO + HO_2 \rightleftarrows CO_2 + OH$*	*0.390E+09*		*103.88*	*36.1*	*0.895E-02*
29	$C_2H_6 \rightleftarrows C_2H_5 + H$	0.500E+17		372.00	-0.9	0.125E-02
30	$C_2H_6 + O_2 \rightleftarrows C_2H_5 + HO_2$	0.400E+08		213.00	3.6	0.441E-04
31	*$C_2H_6 + H \rightleftarrows C_2H_5 + H_2$*	*0.118E-02*	*3.500*	*20.33*	*3.9*	*0.420E-01*
32	*$C_2H_6 + OH \rightleftarrows C_2H_5 + H_2O$*	*0.142E+05*	*1.040*	*7.60*	*6.4*	*0.781E-02*
33	$C_2H_6 + HO_2 \rightleftarrows C_2H_5 + H_2O_2$	0.290E+06		62.50	6.8	0.178E-03
34	*$C_2H_6 + CH_3 \rightleftarrows C_2H_5 + CH_4$*	*0.550E-06*	*4.018*	*34.87*	*3.4*	*0.868E-01*
35	$C_2H_5 + HO_2 \rightleftarrows CH_3 + CH_2O + OH$	0.240E+08		0.00	31.0	0.204E-03
36	*$C_2H_5 + OH \rightleftarrows C_2H_6 + O$*	*0.300E+06*		*25.00*	*-18.2*	*0.193E-09*
37	*$C_2H_5 \rightleftarrows C_2H_4 + H$*	*0.596E+14*		*167.66*	*0.0*	*0.197E+00*
38	*$C_2H_5 + O_2 \rightleftarrows C_2H_4 + HO_2$*	*0.588E+07*		*26.14*	*4.6*	*0.118E+00*
39	*$C_2H_4 + O_2 \rightleftarrows C_2H_3 + HO_2$*	*0.281E+07*		*144.55*	*0.8*	*0.821E-02*
40	*$C_2H_4 + H \rightleftarrows C_2H_3 + H_2$*	*0.150E+09*		*42.70*	*1.1*	*0.123E-01*
41	*$C_2H_4 + O \rightleftarrows C_2H_3 + OH$*	*0.130E+06*	*0.630*	*5.70*	*15.4*	*0.956E-02*
42	*$C_2H_4 + OH \rightleftarrows C_2H_3 + H_2O$*	*0.612E+08*		*24.70*	*3.6*	*0.394E-02*
43	*$C_2H_4 + CH_3 \rightleftarrows C_2H_3 + CH_4$*	*0.199E+07*		*51.46*	*0.6*	*0.378E-01*
44	*$C_2H_4 + O \rightleftarrows CH_3 + CHO$*	*0.127E+03*	*1.489*	*1.80*	*23.0*	*0.577E-02*
45	*$C_2H_4 + OH \rightleftarrows CH_3 + CH_2O$*	*0.830E+07*		*0.00*	*2.2*	*0.887E-02*
46	$C_2H_3 + C_2H_6 \rightleftarrows C_2H_4 + C_2H_5$	0.600E-03	3.300	43.90	2.8	0.183E-03
47	*$C_2H_3 \rightleftarrows C_2H_2 + H$*	*0.121E+16*		*176.44*	*0.0*	*0.233E+00*
48	*$C_2H_3 + O_2 \rightleftarrows C_2H_2 + HO_2$*	*0.198E+06*		*0.00*	*4.5*	*0.121E-01*
49	$C_2H_2 + O_2 \rightleftarrows CHO + CHO$	0.341E+07		143.36	48.7	0.189E-02
50	$O_2 + H \rightleftarrows O + OH$	0.156E+12	0.910	140.85	14.2	0.397E-05
51	*$O_2 + H + M \rightleftarrows HO_2 + M$*	*0.200E+07*	*0.800*	*0.00*	*4.5*	*0.106E-01*
52	$O + HO_2 \rightleftarrows O_2 + OH$	0.200E+08		0.00	14.6	0.905E-05
53	$O + H_2 \rightleftarrows OH + H$	0.150E+02	2.000	31.60	14.3	0.281E-02
54	$O + H_2O \rightleftarrows OH + OH$	0.460E+04	1.300	71.50	11.8	0.172E-03
55	$O + H_2O_2 \rightleftarrows OH + HO_2$	0.631E+07		20.75	11.4	0.141E-05
56	$OH + H_2 \rightleftarrows H_2O + H$	0.100E+03	1.600	13.80	2.5	0.526E-02
57	$OH + H + M \rightleftarrows H_2O + M$	0.220E+11	2.000	0.00	7.3	0.769E-09
58	$OH + HO_2 \rightleftarrows H_2O + O_2$	0.200E+08		0.00	2.8	0.549E-05
59	$OH + H_2O_2 \rightleftarrows H_2O + HO_2$	0.175E+07		1.33	-0.4	0.215E-05
60	$HO_2 + H \rightleftarrows O_2 + H_2$	0.250E+08		2.90	0.3	0.484E-04
61	$HO_2 + HO_2 \rightleftarrows O_2 + OH + OH$	0.200E+07		0.00	24.3	0.430E-03
62	$HO_2 + H_2 \rightleftarrows H_2O_2 + H$	0.300E+08		109.00	2.9	0.370E-03
63	*$OH + OH + M \rightleftarrows H_2O_2 + M$*	*0.320E+11*	*-2.000*	*0.00*	*-21.0*	*0.114E-09*
64	$HO_2 + H \rightleftarrows OH + OH$	0.150E+09		4.20	28.8	0.251E-03
65	$H_2O_2 + H \rightleftarrows OH + H_2O$	0.100E+08		16.60	28.4	0.213E-04
66	$H + H + M \rightleftarrows H_2 + M$	0.180E+07	1.000	0.00	4.9	0.654E-09

[a] Conditions: T_{max} = 1062 K, $CH_4/O_2|_0$ = 10, $He/CH_4|_0$ = 0, and $V/F_{CH_4,0}$ = 0.5 m^3 s mol^{-1}. Affinities and rates calculated at $T = T_{max}$, X_{CH_4} = 3.5%, and X_{O_2} = 35%. Units: A, s^{-1} or m^3 mol^{-1} s^{-1} or m^6 mol^{-2} s^{-1}; E_a, kJ mol^{-1}; $\bar{r}$, mol m^{-3} s^{-1}. Italic characters: reduced model. 0.370E+16 represents 0.370×10^{16}, etc.

(f) (oxy)dehydrogenation of ethane to ethene and ethene to ethyne, reactions 29–43 and 46–48

(g) decomposition of ethene, ethyne, and ethyl radicals, reactions 35, 44, 45, and 49

Table III. Comparison of Typical Experimental Conversions and Selectivities with Those Simulated before and after Regression[a]

	experimental	before regression	after regression: complete network	after regression: reduced network
X_{CH_4}	10.7	7.4	9.6	9.8
X_{O_2}	94.5	62.9	96.8	98.1
S_{CO}	57.9	46.7	56.1	56.3
S_{CO_2}	4.2	26.2	4.3	4.4
$S_{C_2H_4}$	30.4	3.5	30.7	31.2
$S_{C_2H_6}$	7.5	4.3	7.9	7.5

[a] Conditions: T_{max} = 1062 K, $CH_4/O_2|_0$ = 10, inert/$CH_4|_0$ = 0, and $V/F_{CH_4,0}$ = 1.2 m³ s mol⁻¹.

(h) hydrogen–oxygen reactions, reactions 50–66

A common practice in combustion studies is the use of the modified Arrhenius relation for the rate coefficient of the elementary steps, i.e.,

$$k = AT^n \exp(-E_a/RT) \qquad \text{(eq 11)}$$

with three temperature-independent parameters: the activation energy E_a, the preexponential factor A, and the exponent n which accounts for the variations with temperature of the E'_a and A' in the simple Arrhenius relation with two parameters: $k = A' \exp(-E'_a/RT)$. If a linear relation is assumed for the variation of E'_a with temperature:

$$E'_a = E_a + CT \qquad \text{(eq 12)}$$

Integration of

$$E'_a \equiv RT^2(\partial \ln k/\partial T) \qquad \text{(eq 13)}$$

gives

$$\ln k = -\frac{E_a}{RT} + \frac{C}{R} \ln T + \ln C' \qquad \text{(eq 14)}$$

therefore $A = C'$ and $n = C/R$ (Benson, 1976). Combining this effect with the variation of A' yields the values reported in the literature for n, ranging from −2 to 4.

The present work uses for most reactions two-parameter relations. Three-parameter relations are adopted when recommended by Tsang and Hampson (1986). The work from Tsang and Hampson is a very comprehensive compilation and is used as a primary source of the Arrhenius parameters. Other data bases were used as supplements, such as that of Warnatz (1983, 1984), Semenov (1958), and Zanthoff and Baerns (1990).

The rate coefficient for the reverse step was calculated by means of the equilibrium constant and the forward step rate coefficient according to

$$k_{-i} = k_i/K_i \qquad \text{(eq 15)}$$

The equilibrium constant, K_i, is calculated at a measured temperature by using the CHEMKIN thermodynamic data base of the Sandia National Laboratory (Kee et al., 1989).

Simulation results based on the rate coefficients from the literature were not in agreement with the experimental observations. This is illustrated in Table III. In general, the simulated conversions were too low, while the selectivities to CO_x were too high and those to C_2 products were too low. Clearly, the adjustment of some of the parameters is necessary. This was conducted by means of the regression of the experimental data, as described in the Procedures section.

The final parameter estimates after regression are listed in Table II. Before the regression, the parameters to be adjusted were identified by sensitivity and contribution analyses. The reactions of which some parameters have been adjusted during the regression are reactions 2–8, 10 and 11, 21, 23, 28, 31, 32, 34, 37–39, 42–45, 47, and 48. A comparison of parameter estimates after regression with the literature values which were selected as the initial guesses shows that most of the rate coefficients have been changed by factors ranging from 1/5 to 5. The largest change is that of the initiation reaction (2), for which the rate coefficient has been increased by a factor of 20 at 1123 K.

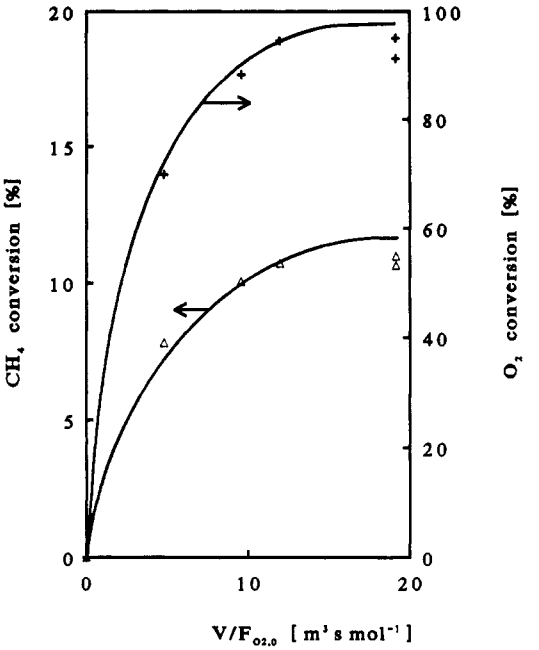

Figure 1. Conversions of methane and oxygen versus space time. Full lines: calculated by integration of eq 5 with the parameter values of Table II. Points, experimental: △, CH_4; +, O_2. T_{max} = 1062 K, $CH_4/O_2|_0$ = 10, and $He/CH_4|_0$ = 0.

In the right half of Table II, the first three columns are the modified Arrhenius parameters for the forward step. The fourth column lists the affinity divided by RT for every reaction. The affinity for a reaction A + B ⇄ P + Q is given by the Gibbs free energy difference of the reaction with the minus sign:

$$A = RT \ln K_i + RT \ln \frac{C_A C_B}{C_P C_Q} = RT \ln \frac{\vec{r}_i}{\overleftarrow{r}_i} \qquad \text{(eq 16)}$$

The value of the affinity of a reaction provides direct information on the direction in which it proceeds and its approach to equilibrium. The values in Table II were calculated at the reactor position corresponding to $T = T_{max}$. At this position the methane and oxygen conversions were about half of their values at the reactor outlet. The outlet conversions were 7% for methane and 70% for oxygen under the reaction conditions referred to in Table II. The last column shows the calculated rate of the forward step at the same position of the reactor and under the same conditions.

Simulation Results

The feed conversions and product selectivities calculated with the parameter estimates reported in Table II are in good agreement with the experimental observations. Figures 1 and 2 show the calculated and experimental conversions of methane and oxygen at two sets of conditions. Figure 1 shows that, at 100% oxygen conversion, the conversion of methane is still far from 15%. However, at the lower CH_4/O_2 inlet ratio corresponding to Figure

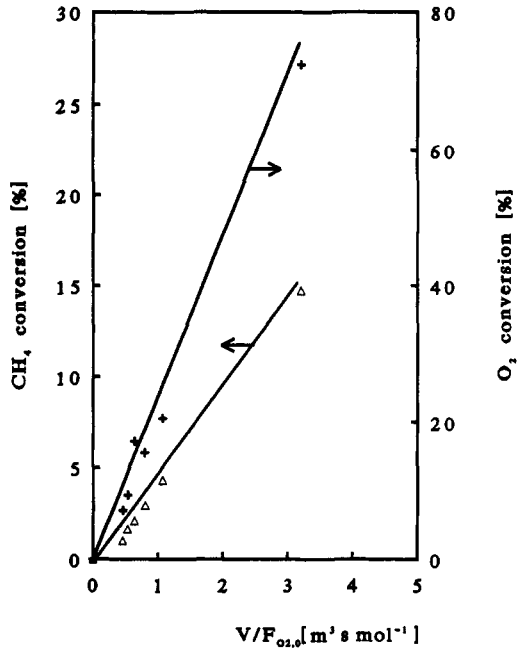

Figure 2. Conversions of methane and oxygen versus space time. Full lines: calculated by integration of eq 5 with the parameter values of Table II. Points, experimental: △, CH_4; +, O_2. T_{max} = 1073 K, $CH_4/O_2|_0$ = 5, and $He/CH_4|_0$ = 1.25.

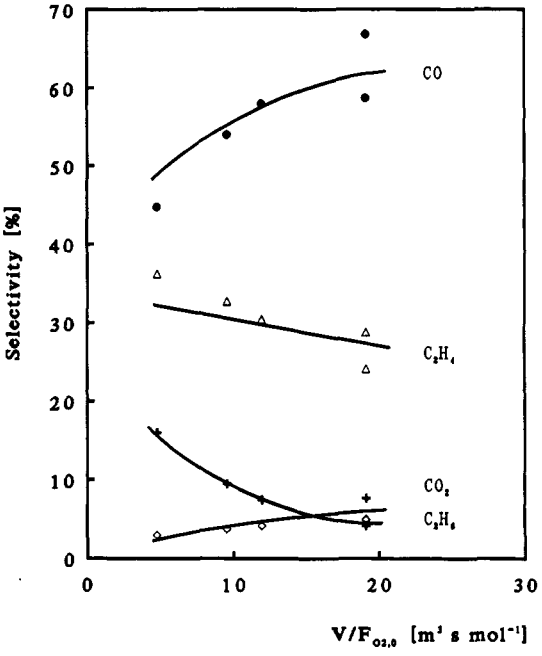

Figure 3. Selectivities for the main reaction products versus space time. Full lines: calculated by integration of eq 5 with the parameter values of Table II. Points, experimental: △, C_2H_4; +, C_2H_6; ●, CO; ◇, CO_2. T_{max} = 1062 K, $CH_4/O_2|_0$ = 10, and $He/CH_4|_0$ = 0.

2, the conversion of methane approaches already 15% at merely 80% oxygen conversion, and at a much shorter space time. At the observed level of selectivities, oxygen is the limiting reactant; hence, higher CH_4/O_2 inlet ratios result in lower methane conversions. Also, lower oxygen partial pressures lead to a lower primary initiation rate, reaction 2 of Table II, and hence, higher space times are required to reach a given conversion. Figure 3 shows the selectivities of some important products versus space time at the set of conditions corresponding to Figure 1. Obviously, the highest C_2 selectivity is attained at the shortest space time, corresponding to low conversion levels. Extrapolation to zero space time indicates, however, a significant direct oxidation of methane to CO. Figure 4 depicts the selectivity versus oxygen conversion. The calculated and experimental product distribution are shown to be in good agreement. In Figure 5, the calculated effect of temperature on feed conversions and selectivities is compared with the observed effect. The temperature here refers to the maximum in the axial temperature profile, denoted as T_{max} in Figures 1–4. At higher temperatures, the calculated C_2 selectivities are a little higher than observed and the opposite is true for CO_x. The effect of

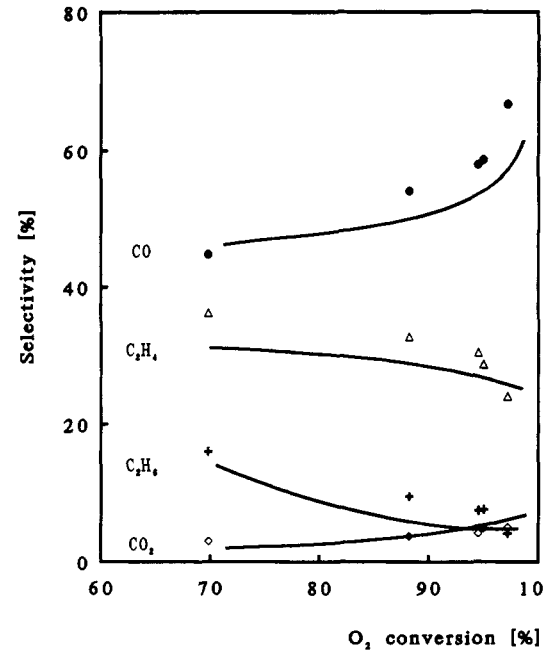

Figure 4. Selectivities for the main reaction products versus oxygen conversion. Full lines: calculated by integration of eq 5 with the parameter values of Table II. Points, experimental: △, C_2H_4; +, C_2H_6; ●, CO; ◇, CO_2. T_{max} = 1062 K, $CH_4/O_2|_0$ = 10, and $He/CH_4|_0$ = 0.

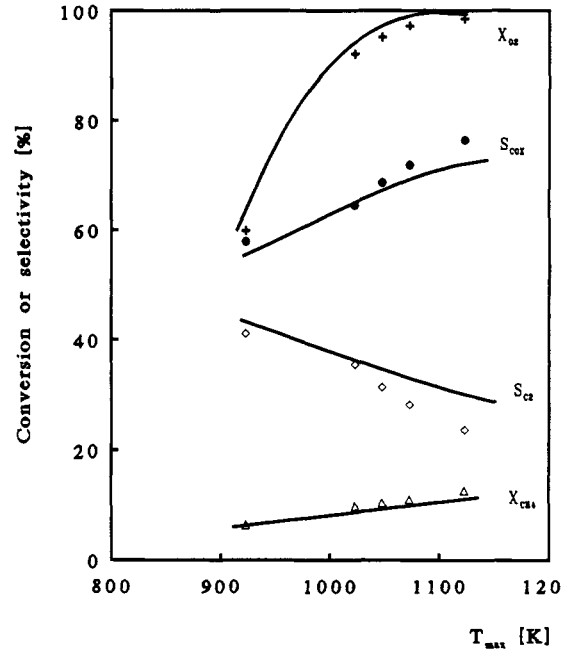

Figure 5. Feed conversions and selectivities for the main reaction products versus the maximum temperature along the reactor. Full lines: calculated by integration of eq 5 with the parameter values of Table II. Points, experimental: △, CH_4 conversion; +, O_2 conversion; ●, C_2 selectivity; ◇, CO_x selectivity. $CH_4/O_2|_0$ = 10 and $He/CH_4|_0$ = 0, $V/F_{CH_4,0}$ = 1.9 m^3 s mol^{-1}.

temperature is most pronounced on the conversion of oxygen, less on the selectivities to C_2 and CO_x, and least on the conversion of methane because of stoichiometric limitations. The selectivity to C_2 decreases with increasing temperature. This indicates that ethane formation via a nonactivated recombination of two methyl radicals is important.

Network Reduction

The contribution analysis performed after the parameter estimation allowed identification of the steps having major contributions to the formation and disappearance of species. On the basis of this information, 44 reactions could be removed without large effects on the simulation, leaving only 33 reactions in a reduced model. Referring to Table II, the reduced model consists of the reactions printed in italics and their corresponding numbers underlined. Note that most reactions typical for pure dihydrogen–dioxygen mixtures, involving H and O atoms and OH and HO_2 radicals, are not important at the conditions investigated, leaving only two of such reactions in the reduced model. All the steps of which some parameters have been adjusted during the regression of the experimental data appear in the reduced model.

The product distribution calculated with the reduced model deviates little from that calculated with the complete model, as can be seen from Table III. The computation time required by the reduced model is about one-third of that required by the complete model. More importantly, since the complexity of the model is reduced, mechanistic insight is increased.

Important Chains

The important chains in the network were assessed by a contribution analysis. The integral contribution factors used in the following sections were calculated with the parameters in Table II. The conditions for the calculation are the same as those used for the calculation of the affinities and rates reported in Table II. The conclusions deduced from the following discussion can be considered as typical for the chains determining the selectivity of the oxidative coupling of methane beyond the primary initiation period.

Chains to Methyl Radicals. The methyl radicals are involved in 23 reactions. More than 90% of the radical is formed in merely three steps. All three reactions in which methyl radicals are formed are hydrogen abstractions from a methane molecule by a radical:

$$CH_4 + H \rightarrow CH_3 + H_2 \quad (3)$$

$$CH_4 + OH \rightarrow CH_3 + H_2O \quad (5)$$

$$CH_4 + HO_2 \rightarrow CH_3 + H_2O_2 \quad (6)$$

while the primary initiation

$$CH_4 + O_2 \rightarrow CH_3 + HO_2 \quad (2)$$

contributes less than 0.1%, and the unimolecular dissociation of methane, (1), even less.

The hydrogen abstraction by the OH radical, (5), accounts for about half of the methyl radical formation. In a recent study of methane oxidation at 728 K and subatmospheric pressure with $CH_4/O_2|_0 = 0.5$, Vedeneev et al. (1990) also concluded that methane disappears predominantly via step 5. More than half of the OH radical is formed in a secondary initiation step

$$H_2O_2 + M \rightarrow 2OH + M \quad (-63)$$

which is fast compared to other initiations. This is a branching step in which a relatively unstable molecule, H_2O_2, gives rise to two OH radicals. Another one-fifth of the OH radicals results from

$$CH_3 + HO_2 \rightarrow CH_3O + OH \quad (10)$$

and less than one-tenth from

$$CH_3 + O_2 \rightarrow CH_2O + OH \quad (8)$$

H_2O_2 originates almost exclusively from step 6. Thus the HO_2 radical is obviously the primary source for OH radicals, taking step 10 also into consideration. The HO_2 radical, in turn, is formed directly from dioxygen, either via step 23 and or via step 38:

$$CHO + O_2 \rightarrow CO + HO_2 \quad (23)$$

$$C_2H_5 + O_2 \rightarrow C_2H_4 + HO_2 \quad (38)$$

The consumption of the OH radicals occurs for more than 90% in step 5 to produce methyl radicals. Therefore, it may be concluded that, at typical methane-coupling conditions, the OH radical generated by a branching step plays a substantial role in generating methyl radicals.

The above can be summarized by two branched chains in Figure 6. The rates of the reverse steps in Figure 6 are negligibly small compared with the forward rates. This can be seen from the values of affinities of the reactions as listed in Table II. Figure 6 shows the dominant chains that lead to the formation of the methyl radical; i.e., steps 5 and 6 account for over three-fourths of the methyl radical production. The global reactions (i) and (ii) can both be considered as branched chains, the common branching step being the decomposition of the hydrogen peroxide. The hydrogen abstractions (5) and (6) and, hence, OH and HO_2 as chain carrier are also common to both chains. In a study of the oxidation of methane by oxygen in the temperature range of 723–800 K, Vardanyan and Nalbandyan (1985) came to similar conclusions concerning the chain branching. They pointed to the decompositions of methyl hydroperoxide and hydrogen peroxide as branching steps. Moreover, they anticipated that the role played by hydrogen peroxide as a chain-branching agent would increase sharply with increasing temperature.

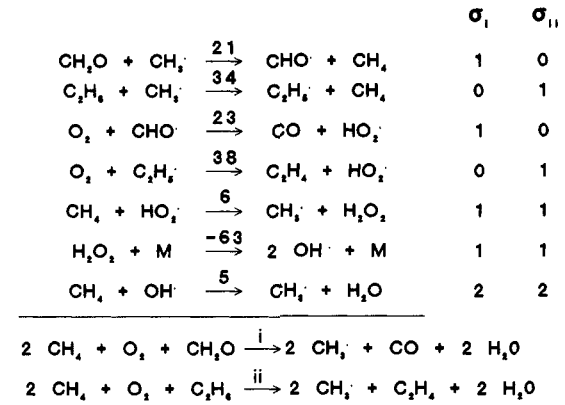

Figure 6. Important chains leading to the production of methyl radicals, two branched chains.

The two chains in Figure 6 have several other features in common. In fact, they are entirely symmetric in terms of the carbon monoxide formation from methanal and ethene formation from ethane, respectively. Both ethane and methanal have positive effects on the methyl radical production. Ethene and carbon monoxide productions accompany the methyl radical generation with C_2H_5 and CHO as corresponding chain carriers.

It is convenient to make the distinction between pyrolysis chains and oxidation chains. The chains in Figure

6 are oxidation chains and account for three-fourths of the methyl radical production. The methyl formation according to (3) represents an example of a step involved in a pyrolytic chain. This step contributes about one-fourth of the formation of the methyl radical. The hydrogen atom is formed mainly in unimolecular radical decompositions, such as

$$CHO + M \rightarrow H + CO + M \quad (22)$$

$$C_2H_3 \rightarrow H + C_2H_2 \quad (47)$$

$$C_2H_5 \rightarrow H + C_2H_4 \quad (37)$$

$$CH_3O \rightarrow H + CH_2O \quad (14)$$

while the rest, less than one-fifth, originates from step −3, i.e., from molecular hydrogen.

Disappearance of Methyl Radicals. The contribution analysis shows that seven steps make up more than 90% of the disappearance of the methyl radical. A termination step, the recombination between two methyl radicals to form ethane, accounts for one-third of its consumption:

$$2CH_3 \rightarrow C_2H_6 \quad (11)$$

Two-thirds of the methyl radicals disappear in chain-propagation steps. In these propagation steps, the methyl radical ends up either in methane, (3), (21), and (34), viz., Figure 6, or in the CO precursors CH_3O and CH_2O, (10), (8), and (7):

$$CH_3 + O_2 \rightarrow CH_3O + O \quad (7)$$

Each of the two pathways consumes about one-third of the total amount of the methyl radicals. Hence, the methyl radical disappearance can roughly be divided into three equal parts: one to ethane, one to CO, and one back to methane. These probabilities of disappearance are in line with the observed selectivities.

For the steps in which they react back to methane, methyl radicals act as a chain carrier. This is essential for the propagation of some chains, particularly those for the formation of carbon monoxide via methanal and for the formation of ethene via ethane, i.e., steps 21 and 34 in Figure 6.

Finally it should be noted that the affinity of reaction 1 is negative. This is consistent with the fact that the

$$CH_4 \rightleftarrows CH_3 + H \quad (1)$$

methyl radical is present in large concentrations. Typically, the highest weight fraction of the methyl radical along the reactor reaches the order of magnitude of 10^{-5} at the conditions of Table II, compared with, e.g., 10^{-8} for the CHO radical and 10^{-9} for the hydrogen atom. The absolute value of the affinity of reaction 1 is close to that of reaction 11, but as the former proceeds much more slowly, the methyl radicals disappear only in a negligibly small fraction via (−1).

Chains to Ethane. Step 11, in which two methyl radicals combine to give ethane, is the major route to ethane, accounting for more than 90% of the total ethane formation. This is generally accepted in the literature (Ito et al., 1985; Zanthoff and Baerns, 1990). Usually, in chain reactions, propagations contribute the most to the product formation. In the oxidative coupling of methane, however, the desired product is yielded in the termination step. In order for this step to be a major contributor to the ethane formation, methyl radicals must be produced by branched chains, as has been discussed previously. On the other hand, in the absence of step 11, the reaction mixture would explode due to the accumulation of the methyl radicals and consequently of the rates of the chains they carry. The

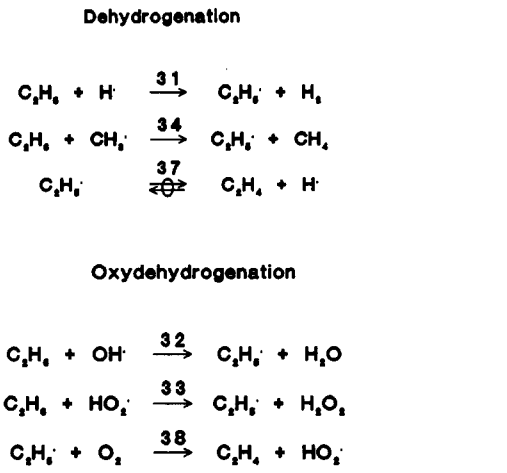

Figure 7. Two most dominant chains for the formation of ethene from ethane.

branched chains are thus degenerated by the termination step (11).

There are also pyrolytic propagation chains leading to ethane, e.g.

$$2CH_3 \rightarrow H + C_2H_5 \quad (12)$$

$$C_2H_5 + CH_4 \rightarrow C_2H_6 + CH_3 \quad (-34)$$

$$CH_4 + H \rightarrow CH_3 + H_2 \quad (3)$$

net: $$2CH_4 \rightarrow C_2H_6 + H_2$$

The contribution analysis shows that less than 0.1% of the ethyl radical itself is produced via the methyl radical substitution step (12). Less than 2% of the formed ethane originates from reaction −34. Hence, the above pyrolytic chain can be neglected. This is due to the high value of the rate coefficient of the nonactivated recombination step (11), which is equal to 1.25×10^7, whereas that of step 12 is smaller by several orders of magnitude, even at 1150 K.

Chains to Ethene. The observed ethene to ethane ratios are well below the equilibrium ratio. Ethene originates from the ethyl radicals, while the contribution of the direct coupling

$$2CH_3 \rightarrow C_2H_4 + H_2 \quad (13)$$

can be neglected. The ethyl radicals are formed almost exclusively from ethane via hydrogen abstractions by various radicals, e.g., H, OH, HO_2, and CH_3.

Figure 7 depicts two routes for the ethene formation from ethane, one pyrolytic and the other oxidative. They include all the principal steps of ethene formation from ethyl radicals and of the ethyl formation from ethane. Similar to the chains shown in Figure 6, the reactions in Figure 7 proceed dominantly to the right. An exception is reaction 37, which is in equilibrium, as is indicated by its affinity. Steps 37 and 38 account for four-fifths of the ethene formation. Steps 31 and 34 plus 32 and 33 together contribute one-third of the ethyl radical formation, with the major contribution coming from the equilibrated reaction step (37). The latter contribution is not relevant, however.

The ethyl radical decompositions to ethene, step 37 in the pyrolytic chain and step 38 in the oxidative chain, proceed at similar rates, viz., Table II. Excluding the equilibrated reaction (37), ethyl radicals are formed for more than three-fourths via the pyrolytic chain, steps 31 and 34, with the rest originating from the oxidative chain. Therefore the pyrolytic chain contributes toward the ethene formation from ethane about three to four times as much as the oxidative chain.

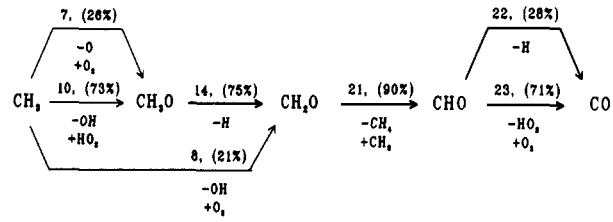

Figure 8. Chains for CO formation from methyl radicals. Numbers in parentheses: integral formation contribution factors. Conditions: T_{max} = 1062 K, $CH_4/O_2|_0$ = 10, $He/CH_4|_0$ = 0, and $V/F_{CH_4,0}$ = 0.5 m^3 s mol^{-1}.

Primary Chains to Carbon Monoxide. The important primary chains leading to the formation of CO from the methyl radical via subsequently CH_3O, CH_2O, and CHO are schematically shown in Figure 8. The chain following the straight arrows in the middle is dominant. Step 21 is clearly the step that all the chains must pass

$$CH_2O + CH_3 \rightarrow CHO + CH_4 \quad (21)$$

through. Methanal is formed for one-fourth from the methyl radical directly via step 8

$$CH_3 + O_2 \rightarrow CH_2O + OH \quad (8)$$

and for three-fourths from CH_3O via step 14. The methyl

$$CH_3O \rightarrow CH_2O + H \quad (14)$$

radicals are the only source of the CH_3O radical which disappears exclusively in step 14. The oxidation of methyl radicals to CH_3O proceeds for one-fourth via step 7 and three-fourths via step 10. Step 7 involves molecular ox-

$$CH_3 + HO_2 \rightarrow CH_3O + OH \quad (10)$$

ygen and, hence, has a high activation energy. It cannot compete with the nonactivated step (10), although the concentration of dioxygen is much larger than that of the HO_2 radical.

Further oxidations of CO yield CO_2. This is the only route through which CO_2 is formed.

Consecutive Oxidation to Carbon Monoxide. In the present model, several reactions for the oxidation of the produced C_2 components to CO are included:

$$C_2H_5 + HO_2 \rightleftarrows CH_3 + CH_2O + OH \quad (35)$$

$$C_2H_4 + O \rightleftarrows CH_3 + CHO \quad (44)$$

$$C_2H_4 + OH \rightleftarrows CH_3 + CH_2O \quad (45)$$

$$C_2H_2 + O_2 \rightleftarrows 2CHO \quad (49)$$

The positive affinities of all these reactions show that they lead to the destruction of C_2 components. Note that the direct oxidation of ethane, analogous to reactions 44, 45, and 49, was not considered in the network because of the higher strength of the C–C bond in ethane compared with ethene and ethyne. Even the indirect oxidation of ethane, i.e., via reaction 35, can be neglected compared to reactions 44, 45, and 49. The fraction of CH_2O and CHO that is formed via the latter reactions, however, amounts to less than one-tenth of their formation via methyl radicals, i.e., reactions 10, 7, and 8. In other words, the unselective oxidation in the methane coupling is mainly due to the methyl radical oxidation, whereas the consecutive oxidation of the hydrocarbon products is not important at the conversion levels investigated.

Relevance of the Oxygen Atom. The importance of the oxygen atom as a chain-branching radical is well established in high-temperature combustion, e.g., the oxidation of hydrogen (Warnatz, 1981, 1983). However, in contrast to this conclusion, the role of the oxygen atom as a major chain-branching radical and thus as a major producer of the methyl radical has not been established from this study. The important chain carrier OH radical is not formed significantly from O atoms through steps 4, 18, -36, 41, and 50. Moreover, the chains with (50) as branching step are not important. The observation of Vardanyan and Nalbandyan (1985) that the peroxides but not the oxygen atom are the chain-branching species agree with the present results. Vedeneev et al. (1990) also pointed out that the O atom is not an important chain-branching species, while the peroxy radicals play an essential role in chain branching.

Conclusions

A detailed kinetic model based on a free-radical mechanism has been developed, which allows the adequate calculation of the feed conversions and product selectivities under process conditions typical for the oxidative coupling of methane. For that matter the available kinetic data bases are not reliable enough, and an estimation of the most important parameters in the model by regression of the experimental data was necessary. The final parameter estimates are physically meaningful.

A contribution analysis allowed revealment of the essential features of the complex reaction network by identifying the important chains. Large amounts of methyl radicals are formed through branched chains, which degenerate via a termination step to produce the desired product ethane. The decomposition of hydrogen peroxide is the main branching step. Ethane (oxy)dehydrogenations lead to ethene. The dehydrogenation via the pyrolytic chain dominates the oxydehydrogenation via the oxidative chain. Carbon monoxide formation is mainly due to the oxidation of the methyl radical at the conversion levels investigated.

Acknowledgment

This work is funded in part by the Commission of the European Communities in the framework of the Joule program, subprogram Energy from Fossil Sources, Hydrocarbons, No. JOUF-0044-C.

Nomenclature

A, B, P, Q = reaction component
A = frequency factor, dependent on n
$\mathcal{A}$ = affinity of a reaction, kJ mol^{-1}
A' = preexponential factor, first-order reaction, s^{-1}; preexponential factor, second-order reaction, m^3 mol^{-1} s^{-1}; preexponential factor, third-order reaction, m^6 mol^2 s^{-1}
$\mathbf{b}$ = parameter vector
C = concentration, mol m^3
d_t = inner diameter of reactor tube, m
E_a = invariant activation energy, kJ mol^{-1}
E'_a = activation energy including contributions of temperature dependence, kJ mol^{-1}
F_j = molar flow rate of component j, mol s^{-1}
$f_j(\mathbf{x}_k,\mathbf{b})$ = calculated response value for response j and experiment k, with the parameter estimates $\mathbf{b}$
ΔH°_r = standard enthalpy of reaction, J mol^{-1}
K = equilibrium constant
k_i = rate constant for a forward step, units the same as A'
k_{-i} = rate constant for a backward step, units the same as A'
m_i = number of oxygen atoms in product i
n = number of experiments; also the third parameter in the modified Arrhenius equation
n_i = number of carbon atoms in product i
R = gas constant, 8.314 × 10^{-3}, kJ mol^{-1} K^{-1}
R_v = volumetric rate of reaction, mol m^{-3} s^{-1}
r_i = rate of reaction i, mol m^{-3} s^{-1}

$\vec{r}_i$ = rate of the forward step of reaction i, mol m^{-3} s^{-1}
$\overleftarrow{r}_i$ = rate of the backward step of reaction i, mol m^{-3} s^{-1}
r^{d}_{ijk} = rate of the disappearance of component j resulting from reaction i in experiment k, mol m^{-3} s^{-1}
r^{f}_{ijk} = rate of the formation of component j resulting from reaction i in experiment k, mol m^{-3} s^{-1}
S = objective function
S_{ij} = selectivity of i with respect to feed j
T = temperature, K
V = reactor volume, m^3
υ = number of responses
w_j = weighting factor of response j
X = conversion of feed component
$\mathbf{x}_k$ = vector of independent variables
y_{kj} = observed values of response j, i.e., molar fraction of component j in experiment k in the objective function
z = length along the reactor, m

Greek Symbols

α_{ij} = reaction order with respect to component j in the forward step of reaction i
α_{-ij} = reaction order with respect to component j in the backward step of reaction i
λ_e = effective heat conductivity, W m^{-1} K^{-1}
σ = stoichiometric number
ν_{ij} = stoichiometric coefficient of component j in reaction i, negative for a reactant and positive for a product
ϕ^{d}_{ijk} = contribution factor of step i toward the disappearance of component j in experiment k
ϕ^{f}_{ijk} = contribution factor of step i toward the formation of component j in experiment k
ψ_{jkl} = sensitivity factor of component j with respect to parameter l in experiment k

Superscripts

d = disappearance
f = formation

Subscripts

0 = reactor inlet
i = index for reaction
j = index for component
k = index for experiment
l = index for parameter
max = maximum
t = reactor tube
v = volumetric

Registry No. CH_4, 74-82-8; C_2H_6, 74-84-0; C_2H_4, 74-85-1; CO, 630-08-0.

Literature Cited

Benson, S. W. *Thermochemical Kinetics*; 2nd ed.; Wiley: New York, 1976; Chapter 1, pp 10–12.

Boudart, M. *Kinetics of Chemical Processes*; Prentice-Hall: Englewood Cliffs, NJ, 1968; Chapter 7, pp 148–152.

Clymans, P. De Produktie van Olefines uit Gasolies en de Rigoureuse Simulatie van de Thermische Kraking. Ph.D. Dissertation, Rijksuniversiteit, Gent, Belgium, 1982.

Dente, M.; Ranzi, E.; Goossens, A. G. Detailed Prediction of Olefin Yields from Hydrocarbon Pyrolysis through a Fundamental Simulation Model (SPYRO). *Comput. Chem. Eng.* **1979**, *3*, 61–75.

Froment, G. F.; Hosten, L. H. Catalytic Kinetics: Modeling. In *Catalysis: Science and Technology*; Anderson, J. R., Boudart, M., Eds.; Springer Verlag: Berlin, 1981.

Gear, C. W. The Automatic Integration of Ordinary Differential Equations. *Commun. ACM* **1971**, *14*, 176.

Geerts, J. W. M. H.; Chen, Q.; Van Kasteren, J. M. N.; Van Der Wiele, K. Thermodynamics and Kinetic Modeling of the Homogeneous Gas Phase Reactions of the Oxidative Coupling of Methane. *Catal. Today* **1990**, *6*, 519.

Hindmarsh, A. C. ODEPACK, A Systemized Collection of ODE Solvers. In *Scientific Computing: Applications of Mathematics and Computing to the Physical Sciences*; Stepleman et al., Eds.; IMACS Transactions on Scientific Computing 1; North Holland: Amsterdam, 1983.

Ito, T.; Wang, J.-X.; Lin, C.-H.; Lunsford, J. H. Oxidative Dimerization of Methane over a Lithium-Promoted Magnesium Oxide Catalyst. *J. Am. Chem. Soc.* **1985**, *107*, 5062.

Kee, R. J.; Rupley, F. M.; Miller, J. A. "The CHEMKIN Thermodynamic Data Base"; Sandia Report SAND87-8215.UC-4; Reprinted April 1989.

Kimble, J. B.; Kolts, J. H. Playing Matchmaker with Methane. *CHEMTECH* **1987**, *Aug*, 501.

Labinger, J. A.; Ott, K. C. Mechanistic Studies on the Oxidative Coupling of Methane. *J. Phys. Chem.* **1987**, *91*, 2682.

Lane, G. S.; Wolf, E. E. Methane Utilization by Oxidative Coupling I. A Study of Reactions in the Gas Phase during the Cofeeding of Methane and Oxygen. *J. Catal.* **1988**, *113*, 144.

Lunsford, J. H. The Catalytic Conversion of Methane to Higher Hydrocarbons. *Catal. Today* **1990**, *6*, 235.

Mears, D. E. Diagnostic Criteria for Heat Transport Limitations in Fixed Bed Reactor. *J. Catal.* **1971**, *20*, 127–131.

NAG. *FORTRAN Library Manual-Mark* 13; Oxford, 1988; Vol. 2.

Rosenbrock, H. H. An Automatic method for Finding the Greatest or Least Value of a Function. *Comput. J.* **1961**, *3*, 175–184.

Rosenbrock, H. H.; Story, C. *Computational Techniques for Chemical Engineers*; Pergamon Press: Oxford, 1966.

Semenov, N. *Some Problems in Chemical Kinetics and Reactivity*. Translated from Russian by Boudart, M.; Princeton University Press: Princeton, NJ, 1958.

Skinner, G. B.; Lifshitz, A.; Scheller, K.; Burca, A. Kinetics of Methane Oxidation. *J. Chem. Phys.* **1972**, *56*, 3853.

Sundaram, K. M.; Froment, G. F. Modeling of Thermal Cracking Kinetics. 3. Radical Mechanism for the Pyrolysis of Simple Paraffins, Olefins, and Their Mixtures. *Ind. Eng. Chem. Fundam.* **1978**, *17*, 174.

Tsang, W.; Hampson, R. F. Chemical Kinetic Database for Combustion Chemistry. Part I, Methane and Related Compounds. *J. Phys. Chem. Ref. Data* **1986**, *15*, 1087.

Van Kasteren; H. M. N.; Geerts, J. W. M. N.; Van Der Wiele, K. Ethylene Synthesis by Catalytic Oxidation of Methane over Li-doped MgO catalysts: The Interaction of Catalytic and Non-Catalytic Reaction Steps. *Proc. Ninth Int. Congr. Catal.* **1988**, *2*, 930.

Vardanyan, I. A.; Nalbandyan, A. B. On the Mechanism of Thermal Oxidation of Methane. *Int. J. Chem. Kinet.* **1985**, *17*, 901.

Vedeneev, V. I.; Karnaukh, A. A.; Mantashyan, A. A.; Teitel'boim, M. A., Mechanism of Chain Propagation in the Oxidation of Methane. *Kinet. Catal.* **1990**, *31*, 1.

Warnatz, J. Chemistry of Stationary and Non-Stationary Combustion. In *Modelling of Chemical Reaction Systems*; Ebert et al., Eds.; Springer Verlag: Berlin, 1981.

Warnatz, J. Hydrocarbon Oxidation at High Temperatures. *Ber. Bunsen-Ges. Phys. Chem.* **1983**, *87*, 1008.

Warnatz, J. Rate Coefficients in the C/H/O system. In *Combustion Chemistry*; Gardiner, W. C., Ed.; Springer Verlag: New York, 1984; Chapter 5.

Zanthoff, H.; Baerns, M. Oxidative Coupling of Methane in the Gas Phase. Kinetic Simulation and Experimental Verification. *Ind. Eng. Chem. Res.* **1990**, *29*, 2.

Received for review January 2, 1991
Revised manuscript received April 17, 1991
Accepted May 9, 1991